Neuropeptides 53 (2015) 51–62

Contents lists available at ScienceDirect

Neuropeptides

journal homepage: www.elsevier.com/locate/ynpep

Kinin B2 receptor can play a neuroprotective role in Alzheimer's disease

A.L. Caetano [a,e], K.E. Dong-Creste [a,e], F.A. Amaral [a], K.C. Monteiro-Silva [a], J.B. Pesquero [c], M.S. Araujo [d], W.R. Montor [a], T.A. Viel [b,e,1], H.S. Buck [a,e,*,1]

[a] Department of Physiological Sciences, Santa Casa de Sao Paulo School of Medical Sciences, Sao Paulo, SP CEP 01221-020, Brazil
[b] School of Arts, Sciences and Humanities and Graduation Course on Pharmacology at Institute of Biomedical Sciences, University of Sao Paulo, Sao Paulo, SP CEP 03828-080, Brazil
[c] Department of Biophysics, Federal University of Sao Paulo, São Paulo, SP CEP 04021-001, Brazil
[d] Department of Biochemistry, Federal University of Sao Paulo, São Paulo, SP CEP 04021-001, Brazil
[e] Research Group on Neuropharmacology of Aging, Brazil

ARTICLE INFO

Article history:
Received 2 December 2014
Received in revised form 4 September 2015
Accepted 5 September 2015
Available online 19 September 2015

Keywords:
Bradykinin
B2 receptor
Alzheimer's disease
Amyloid beta
Knockout mice

ABSTRACT

Alzheimer's disease (AD) is characterized by cognitive decline, presence of amyloid-beta peptide (Aβ) aggregates and neurofibrillary tangles. Kinins act through B1 and B2 G-protein coupled receptors (B1R and B2R). Chronic infusion of Aβ peptide leads to memory impairment and increases in densities of both kinin receptors in memory processing areas. Similar memory impairment was observed in C57BL/6 mice (WTAβ) but occurred earlier in mice lacking B2R (KOB2Aβ) and was absent in mice lacking B1R (KOB1Aβ). Thus, the aim of this study was to evaluate the participation of B1R and B2R in Aβ peptide induced cognitive deficits through the evaluation of densities of kinin receptors, synapses, cell bodies and number of Aβ deposits in brain of WTAβ, KOB1Aβ and KOB2Aβ mice. An increase in B2R density was observed in both WTAβ and KOB1Aβ in memory processing related areas. KOB1Aβ showed a decrease in neuronal density and an increase in synaptic density and, in addition, an increase in Aβ deposits in KOB2Aβ was observed. In conclusion, memory preservation in KOB1Aβ, could be due to the increase in densities of B2R, suggesting a neuroprotective role for B2R, reinforced by the increased number of Aβ plaques in KOB2Aβ. Our data point to B2R as a potential therapeutic target in AD.

1. Introduction

The oligopeptides bradykinin (BK) and kallidin, also called Lys-BK, are released in the plasma or interstitial fluid after the cleavage of kininogens by kallikreins and their effects are the result of the activation of two G-protein coupled transmembrane receptors, called B1 and B2 (B1R and B2R, respectively) (Regoli and Barabe, 1980). The B2R is a constitutive receptor, its stimulation leading to a fast desensitization (Smith et al., 1995; Bascands et al., 1993; Mathis et al., 1996). It mediates most of kinin actions and has high affinity for BK and high sensitivity to low concentrations of the synthetic antagonist HOE 140 (Regoli et al., 1998). Conversely, B1R has higher affinity to des-Arg9BK and Lys-des-Arg9-BK (Regoli and Barabe, 1980). B1R is resistant to desensitization and is barely distributed in tissues under physiological conditions (Leeb-Lundberg et al., 2005), but shows increased densities under pathological conditions, such as chronic neurological diseases (Marceau et al., 1998; Prat et al., 1999; Prat et al., 2000).

When administered in the central nervous system (CNS), BK leads to behavioral effects as initial excitation followed by sedation (Okada et al., 1977), electroencephalographic desynchronization (Kariya and Yamauchi, 1981), increase in arterial blood pressure and reduction of diuresis (Hoffman and Schimid, 1978; Fior et al., 1993; Lindsey et al., 1997; Cloutier et al., 2002). In the rat hippocampus, a single dose of BK promotes hyperphosphorylation of the Tau protein eliciting memory and learning impairment (Wang and Wang, 2002). Kinin B2R is widely distributed in the CNS, being described in several nuclei of rats (Cholewinski et al., 1991; Couture and Lindsey, 2000; Viel et al., 2008), mice (Ma et al., 1994a), guinea pigs (Lopes et al., 1983; Sharif and Whiting, 1991; Murone et al., 1997; Fujiwara et al., 1988), bovine cattle (Kozlowski et al., 1998) and humans (Ma et al., 1994b; Raidoo et al., 1996) as assessed by RT-PCR, immunohistochemistry and autoradiography.

Alzheimer's disease (AD) is a progressive neurodegenerative disease with severe impact on learning and memory. This disease is neurohistopathologically characterized by ultra-structural lesions and the formation of senile plaques, composed of amyloid-β peptide (Aβ) deposits, and neurofibrillary tangles, formed by hyperphosphorylation of tau-protein filaments.

In vitro studies showed an increased production of inositol triphosphate (IP3) after stimulation of BK in skin fibroblasts obtained from patients with familial AD but not in fibroblasts obtained from sporadic AD patients (Huang et al., 1995). Furthermore, a pharmacodynamic modulation of BK receptors and an increase in the phosphorylation of

* Corresponding author at: Department of Physiological Sciences, Santa Casa de Sao Paulo School of Medical Sciences, Rua Dr. Cesário Motta Junior, 61, Sao Paulo, SP CEP 01221-020, Brazil.
[1] These authors contributed equally to this work.

http://dx.doi.org/10.1016/j.npep.2015.09.001
0143-4179/

various proteins were observed in a cellular model of AD, after stimulation with BK (Jong et al., 2002; Zhao et al., 2002).

Our group showed significant neuronal loss and amyloid deposit formation in the cortex and the hippocampus and an increase in kinin concentration in the cerebrospinal fluid in rats infused with human 1–40 Aβ peptide (Iores-Marçal et al., 2006), suggesting an enhanced activation of the kallilkrein–kinin-system (KKS) (Iores-Marçal et al., 2006). Moreover, we showed a disruption in memory consolidation of rats submitted to the same protocol, accompanied by an increase in B1R densities in the ventral hippocampal commissure, fimbria, CA1 and CA3 hippocampal areas, habenular nuclei and optical tract, when compared to the correlated areas in the control group. The most remarkable observation was a significant increase of B2R densities in brain nuclei related to cognitive process and the absence of labeling in the same areas from the control group (Viel et al., 2008). Recently we showed changes in memory processing of B1R or B2R knockout mice (KOB1, KOB2) after i.c.v. chronic infusion of human 1–40 Aβ peptide. KOB2 mice showed early memory disruption when compared to C57Bl/6 animals suggesting that B2R may play a neuroprotective role. Besides, KOB1 mice showed no memory deficits, suggesting that the absence of B1R apparently prevented the cognitive deficit normally observed at the end of the infusion period (Amaral et al., 2010; Viel and Buck, 2011). Considering that normal receptor regulation can be altered by the absence of B1R or B2R in knockout animals the aim of this work was to evaluate the expression of B1R in KOB2 mice and of B2R in KOB1 mice, as well as the neuronal plasticity in these animals after i.c.v. chronic infusion of human 1–40 Aβ peptide (treated group) in comparison to the vehicle group (control group).

2. Material and methods

2.1. Tissue preparation

Brain samples were obtained from C57Bl/6 (wild type, WT), KOB1 and KOB2 mice, 28–31 g of body weight, 12 weeks of age, provided from our own breeding colony. Animals were kept in controlled room temperature (22–24 °C) and humidity (55–65%), with food and water *ad libitum* in a 12 h light/dark cycle. All surgery and care procedures were performed according to the guidelines for animal experimentation as stipulated in the Guide for the Care and Use of Laboratory Animals (National Institute of Health Publication No. 86–23, Bethesda, MD) and The Ethics Committee on Experimental Research from Santa Casa de Sao Paulo Medical School. All efforts were made to minimize the number of animals used and their level of suffering. In order to follow that, samples used in this paper are from animals used in a previous study describing the memory alterations of kinin receptors knockout mice after Aβ peptide infusion (Amaral et al., 2010), as described below.

The following method was described in a previous work from our research team, where the behavioral analysis of these animals was reported (Amaral et al., 2010). Briefly, mice were infused with Aβ peptide or vehicle (V) for 35 days in the lateral cerebral ventricle. Knockouts (KOB1Aβ, KOB1V; KOB2Aβ, KOB2V) and WT (WTAβ and WTV) were submitted to surgery for the implantation of mini-osmotic pumps (Alzet, model 1004, Cupertino, CA, USA) filled up with either the vehicle (4 mMHEPES, pH 8.0 — control group) plus 0.22 nmol E-64 (cystein protease inhibitor) or human (1–40) Aβ peptide (0.46 nmol — Aβ group) plus 0.22 nmol E-64. At the end of the infusion period, the animals were introduced into a chamber saturated with CO_2 until they became slightly unconscious (about 2 s) and were immediately killed by decapitation. The brains were immediately removed and frozen in 2-methylbutane cooled at −45 to −55 °C in dry ice, then stored at −80 °C until use. Serial sections of the tissues (20 μm) were cut on a cryostat chamber (−18 to −20 °C, Microm HM 505N, Francheville, France), thaw mounted on gelatin coated slides, desiccated for 5 min at room temperature and kept at −80 °C until use.

Peptide iodination was performed following a method described elsewhere with some modifications (Hunter and Greenwood, 1962; de Sousa Buck et al., 2002). Briefly, 5 μg of B1 antagonist HPP-[desArg10]-HOE 140 or B2 antagonist HPP-HOE 140 was incubated in 0.05 M phosphate buffer for 30 s in the presence of 0.5 mCi (18.5 MBq) of $Na^{125}I$ and 220 nmol of chloramine T in a total volume of 55 μL at room temperature. The reaction was interrupted by 20 μL of 13 mM sodium metabisulfite. The monoiodinated peptide was immediately purified by gel filtration on a Sephadex-G25 column (13 mL) equilibrated in 0.5% bovine serum albumin in 0.1 M acetic acid. The specific activity of the iodinated peptides was calculated to be approximately 2000 cpm/fmol or 1212 Ci/mmol based on the purity of the monoiodinated compound (>95%), determined by reversed phase HPLC.

2.2. Autoradiography for B1 and B2 receptors

This method was based on a procedure described elsewhere (Ongali et al., 2003a; Ongali et al., 2003b; Viel et al., 2008; Caetano et al., 2010). The concentration of radioligands corresponds to maximal specific binding on the saturation curves (Bmax) and was determined on the basis of previous studies (Murone et al., 1997; Ongali et al., 2003a; Ongali et al., 2003b; Cloutier et al., 2004). Briefly, slides were incubated for 90 min at room temperature using 150 pM of iodinated kinin B1 antagonist for the identification of B1R or 200 pM of iodinate kinin B2 antagonist for the identification of B2R. The non-specific binding was determined by simultaneous incubation using 2 μM of the respective unlabelled peptides. After the incubation, sections were exposed against Hyperfilm-MP (double-coated,24 cm × 30 cm, Amersham Biosciences, GEHealthcare, Uppsala, Sweden) for 72 h to 96 h at room temperature, along with autoradiographic [^{125}I] microscales containing predetermined amounts of radioactivity in nCi/mg of tissue prepared as previously described (Nazarali et al., 1989). At the end of exposure time films were developed following manufacturer instruction and the autoradiograms quantified using the MCID image analysis system (Interfoccus Europe, UK). For each animal, 6–10 sections were analyzed. The specific binding was obtained by subtracting the non-specific binding (< 5%) from the total binding from similar adjacent sections. Results were expressed as fmol of iodinated antagonist per mg of tissue (fmol/mg of tissue).

2.3. Immunohistochemical procedure

Slides containing 20 μm frozen slices were warmed at room temperature until they became totally dry and then were fixed with acetone at −20 °C for 5 min at room temperature. After that, they were rapidly washed three times in 0.1 M phosphate buffer saline (PBS) and incubated for 20 min in 0.3% hydrogen peroxide in methanol (300 mL) to quench endogenous peroxidases. Slides were then washed three times in PBS and were incubated for 30 min in 10% normal goat serum (NGS) in PBS to prevent nonspecific staining. Following that, they were incubated with primary antibodies: anti-synaptophysin polyclonal antibody (1:1000; ab68851, Abcam, during 6 h) to evaluate the density of synaptic terminals and anti-NeuN antibody (1:2000, Millipore ABN78, incubated for 2 h) to evaluate neuronal density. After incubation with antibodies, tissues were processed with avidin–biotin complex (Vectastain Elite ABC Kit, Rabbit IgG, PK-6101, Vector Laboratories, Burlingame, CA, USA) according to the manufacturer's instruction. Following this, the immune complex was visualized with 0.05% 3,39-diaminobenzidine tetrahydrochloride (Sigma-Aldrich, St. Louis, MO, USA) plus 0.015% H_2O_2 in 0.01 M PBS, pH 7.2, for 4 min and 30 s exactly. Careful washing in water twice stopped the reaction. All antibodies, the avidin–biotin complex and detection solutions were diluted in PBS with 10% NGS to reduce nonspecific binding. At the end, slices were dehydrated in an ethanol series (50, 75, 95, 100%) cleared in xylene, mounted in “Entellan” (Merck, Darmstadt) and covered with a coverslip. The specificity of synaptophysin and NeuN

immunostainings was determined by the absence of any staining in the lack of either primary or secondary antibodies. Each processed batch contained slides from the different groups.

2.4. Quantification of immunostainings

Immunostainings were analyzed in three areas related to memory function, CPu (Caudate and Putamen), cortex and hippocampus, for the density of immunoreactivity. A segment of 20–22 slices was equally distributed along the interval of 2.80 to −4.16 mm from Bregma (Franklin and Paxinos, 2008). Non-specific labeling was assessed in slices processed in the absence of primary antibody and was used to define background staining. A microcomputer-based image analysis system (MCID; Imaging Research, Interfocus Europe, UK) was used to calculate the proportion of the stained area to the total test area (proportional area = stained area/total test area). Images were thresholded in order to obtain all areas containing DAB reactions in black and the background in white. Threshold levels were individually set for each batch of tissue processed to ensure that all immunoreactivity was identified. Also, threshold and light levels were unchanged in slides of a batch. Values from each section were averaged for each animal, and a mean was determined across animals. Comparisons were performed between treated and control group for each strain and among strains.

2.5. Counting of Aβ deposits

Slides containing 20 μm frozen slices were warmed at room temperature until they became totally dry and were then fixed (5 min) in 4.0% buffered paraformaldehyde and stained by Harrys'hematoxylin and Congo red dye for detection of Aβ deposits. Histological analysis was made using a Nikon Eclipse E600 light microscope (Kanagawa, Japan). Per animal, 20–22 sections were analyzed at an interval of 2.80 to −4.16 mm from bregma (Franklin and Paxinos, 2008), in which all amyloid deposits found were counted. The total number of deposits per animal was divided by the number of slices, establishing a relationship between the number of deposits by the number of sections. This proportion was used for statistical analysis.

2.6. Statistical analysis

Results were expressed as mean ± S.E.M. Differences between B1 and B2 receptor densities at each nuclei were assessed by Student-t test. Data from immunohistochemistry assays were analyzed using two-way ANOVA followed by Bonferroni test. For counting of Aβ deposits, one-way ANOVA was used followed by Tukey-Kramer test. Only probability values (P) less than 0.05 were considered statistically significant.

3. Results

3.1. Localization and quantification of kinin receptors

A quantitative anatomical analysis of autoradiograms from C57Bl/6 (WT), KOB1 and KOB2 (n = 6 each) either infused with vehicle (V) or amyloid-β peptide (Aβ) showed undetectable specific binding sites for the B1 iodinated antagonist [^{125}I]HPP-[des-Arg10]-HOE 140 (data not shown). However, using the B2 iodinated antagonist [^{125}I]HPP-HOE 140 as radioligand to quantify and localize kinin B2 receptors in brains of WT and KOB1 mice, specific binding sites were verified all over the tissue. When comparing the different strains and treatments it was observed that the anatomical distribution of B2 receptor is similar among them (Table 1).

Table 1
Distribution of specific binding of [^{125}I]HPP-HOE 140 to kinin B2 receptors in the brain of C57Bl/6 and KOB1 mice infused with either vehicle or amyloid-β peptide. Abbreviations are described in the legend of Fig. 2.

	KOB1		WT	
	Vehicle	Aβ	Vehicle	Aβ
aca	1.14 ± 0.36	1.68 ± 0.35*	1.02 ± 0.44	1.62 ± 0.42*
Broca's area				
VDB	0.93 ± 0.24	1.61 ± 0.23*	0.68 ± 0.29	0.74 ± 0.22
Septal lateral area				
MS	0.97 ± 0.17	1.69 ± 0.18*	0.41 ± 0.18	0.87 ± 0.39*
Corpus callosum				
ec	0.85 ± 0.30	1.28 ± 0.29*	0.97 ± 0.62	1.08 ± 0.50
ic	0.58 ± 0.24	1.38 ± 0.29*	0.99 ± 0.65	0.93 ± 0.49
fmi	0.25 ± 0.36	1.57 ± 0.05*	0.19 ± 0.26	0.88 ± 0.35*
fmj	0.50 ± 0.09	0.95 ± 0.13*	0.32 ± 0.39	1.46 ± 0.07
cg	0.68 ± 0.29	1.11 ± 0.29*	0.86 ± 0.56	1.00 ± 0.39
Cortex and piriform cortex				
Cortex	0.49 ± 0.15	0.77 ± 0.23*	0.60 ± 0.42	0.49 ± 0.21
Piriform cortex	1.91 ± 0.46	2.49 ± 0.54*	1.71 ± 0.24	1.92 ± 0.54
CPu/SIB				
Cpu	0.44 ± 0.20	0.79 ± 0.21*	0.55 ± 0.37	0.45 ± 0.28
SIB	0.57 ± 0.28	1.59 ± 0.19*	0.55 ± 0.29	0.28 ± 0.08
Hippocampus				
CA1	0.30 ± 0.15	0.35 ± 0.11*	0.25 ± 0.30	0.26 ± 0.16
CA2	0.32 ± 0.16	0.44 ± 0.14*	0.17 ± 0.23	0.28 ± 0.11
CA3	0.31 ± 0.14	0.68 ± 0.40*	0.41 ± 0.38	0.27 ± 0.13
fi	0.45 ± 0.14	1.08 ± 0.15*	0.90 ± 0.60	0.59 ± 0.20
dhc	0.60 ± 0.19	1.14 ± 0.40*	0.78 ± 0.66	0.93 ± 0.52
GrDG	0.32 ± 0.11	0.44 ± 0.13*	0.31 ± 0.31	0.44 ± 0.27
DS	0.38 ± 0.09	0.52 ± 0.08*	0.47 ± 0.43	0.64 ± 0.49
Thalamic nuclei				
PO	0.80 ± 0.31	1.73 ± 0.18*	0.96 ± 0.56	0.78 ± 0.24
VPL	0.69 ± 0.32	1.60 ± 0.17*	1.05 ± 0.67	0.84 ± 0.02
VPM	0.79 ± 0.34	1.65 ± 0.13*	1.24 ± 0.76	0.87 ± 0.12
geniculate n	1.06 ± 0.29	1.42 ± 0.41*	0.98 ± 0.69	0.95 ± 0.39
ZIV/ZID	1.04 ± 0.22	1.63 ± 0.42*	1.07 ± 0.66	1.11 ± 0.50
Hypothalamic nuclei				
Hypothalamic n	0.59 ± 0.29	0.95 ± 0.24*	0.94 ± 0.54	0.88 ± 0.23
PH	0.85 ± 0.09	1.42 ± 0.50*	1.25 ± 0.36	1.53 ± 0.18
PAG				
PAG	1.02 ± 0.26	1.32 ± 0.38*	1.29 ± 0.78	1.15 ± 0.56

* Statistical differences ($p < 0.05$) between Aβ and Vehicle for each strain.

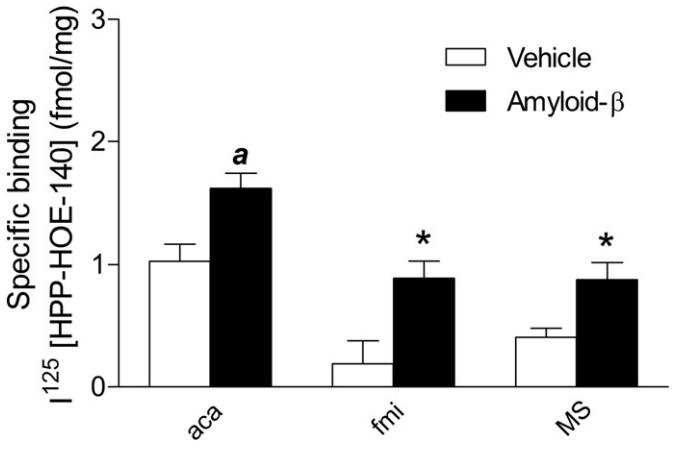

Fig. 1. Quantification of Kinin B2 receptors in WT mice. Specific binding of [^{125}I]HPP-HOE 140 (200 pM, 90 min, room temperature) to B2 bradykinin receptors in different brain areas from Vehicle (blank bars, n = 6) and amyloid-β (dark bars, n = 6) of C57Bl/6 mice groups. Data are expressed as mean ± S.E.M. *$P < 0.05$; $^{a}P < 0.01$. Abbreviation: anterior commisure, anterior part, aca; forceps minor of the corpus callosum, fmi and medial septal nucleus, MS.

3.2. Autoradiography for kinin B2 receptors in wild type mice (WT)

Specific biding sites for the B2 antagonist were spread in areas composing the corpus callosum, hippocampus, hypothalamic nuclei, posterior hypothalamic nucleus, thalamic nuclei, caudate putamen, substantia innominata, nucleus of the ventricular limbo of the diagonal band, periaqueductal gray, anterior part of the anterior commissure, cortex and piriform cortex (Figs. 1 and 2A–D,Table 1).

WTAβ showed significant increase in specific binding sites for B2 antagonist in the anterior part of the anterior commissure, forceps minor of the corpus callosum and medial septal nucleus when compared to WT vehicle group (Figs. 1 and 2A–D, Table 1).

3.3. Autoradiography for kinin B2 receptors in knockout B1 mice (KOB1)

Significant increase of specific binding sites was observed in many brain areas such as the corpus callosum, hippocampus, hypothalamic nuclei, posterior hypothalamic nucleus, thalamic nuclei, caudate putamem, substantia inominata, nucleus of the ventricular limbo of the diagonal band, periaqueductal gray, anterior part of anterior commisure, cortex and piriform cortex (Figs. 3 and B and 2E–H, Table 1).

When compared to the vehicle group, knockout B1 mice showed increased B2R antagonist specific binding sites in all labeled areas, after chronic infusion of Aβ peptide.

Neuronal Nuclei Protein (NeuN) and Synaptophysin Protein quantifications.

For these two proteins, three areas related to memory function were analyzed: CPu, cortex and hippocampus. Concerning NeuN labeling in WT group, the infusion of Aβ promoted a significant decrease of 51.0% in NeuN density in CPu ($P < 0.05$) and 39.3% in the cortex ($P < 0.001$), when compared to the proportional area occupied by NeuN labeling in animals infused with vehicle ($25.3 \pm 15.5\%$ and $22.1 \pm 9.0\%$, respectively). In KOB1 animals, the infusion of Aβ promoted significant decrease of 58.1% in CPu ($P < 0.01$) and 55.0% in hippocampus ($P < 0.05$), when

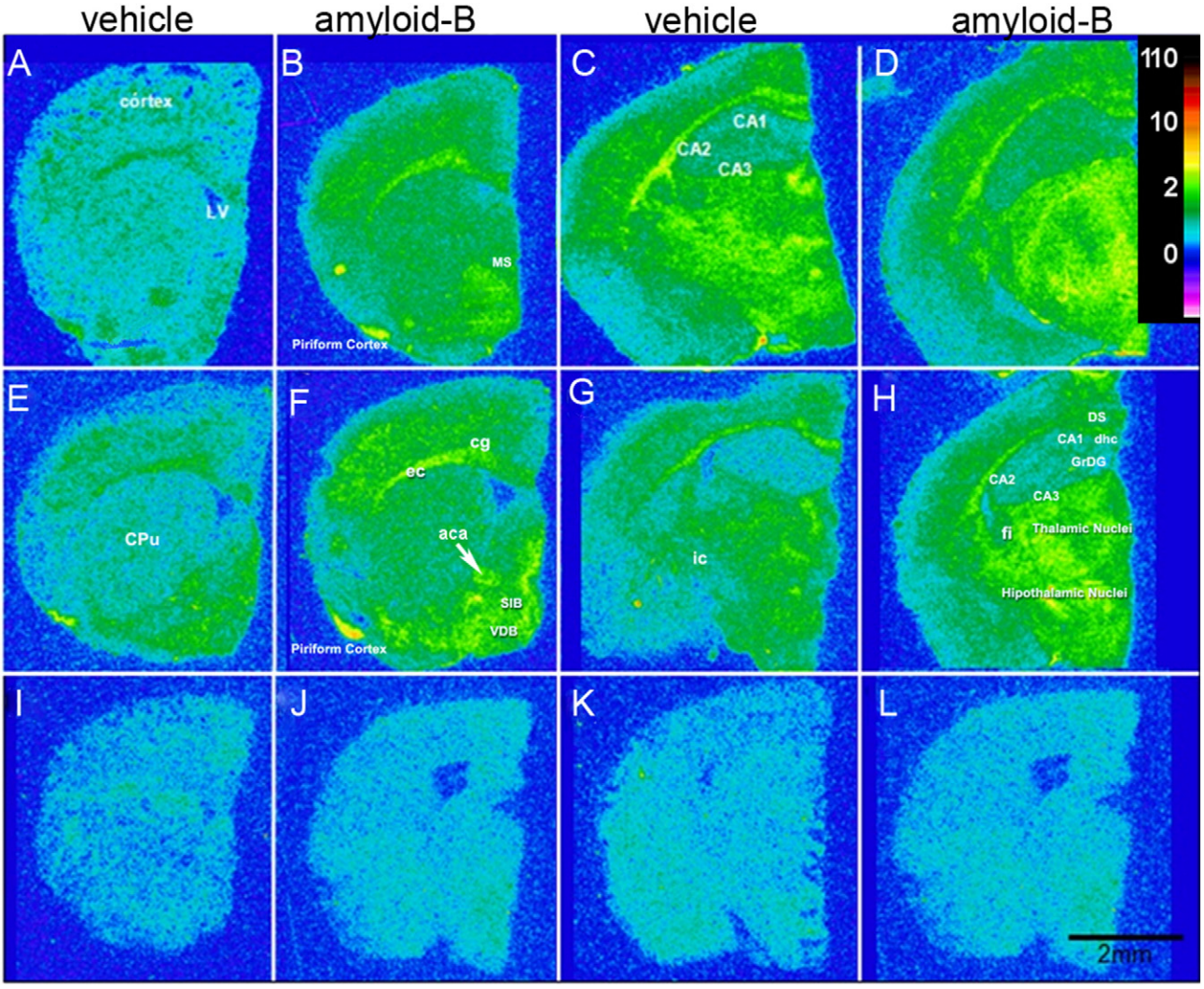

Fig. 2. Anatomical distribution of Kinin B2 receptors. Pseudocolor photomicrographs of autoradiograms representing anatomical distribution of total binding sites for B2 receptor in brains of C57Bl/6 mice (upper panels) and KOB1 mice (middle panels). High level binding of the antagonist to the B2 receptor is shown in yellow, according to the scale in fmol of protein per milligram of tissue. Non-specific binding sites are represented in lower panels. Image analyses were based on the same sections stained with Harry's hematoxylin. The antero-posterior levels are approximately 0.86 mm for "A", "B", "E", "F", "I" and "J" and −2.18 mm for "C", "D", "G", "H", "K" and "L" with reference to the bregma (Franklin and Paxinos, 2008). Abbreviation: external capsule, ec; internal capsule, ic; forceps minor of the corpus callosum, fmi; forceps major of the corpus callosum, fmj; cingulum, cg; CA2 and CA3 hippocampal areas; caudate putamem, CPu; fimbria, fi; dorsal hippocampal commissure, dhc; granule cell layer of the dentate gyrus, GrDG; dorsal subiculum, DS; hypothalamic nuclei, Hn; posterior hypothalamic nucleus, PH; posterior thalamic nuclei, PO; ventral posterolateral thalamic nucleus, VPL; ventral posteromedial thalamic nucleus, VPM; geniculate nuclei, Gn; ventral and dorsal incert zone, ZIV/ZID; medial septal nucleus, MS; substance inominata, SIB; nucleus of the ventricular limbo of the diagonal band, VDB; periaqueductal gray, PAG; anterior commisure, anterior part, aca; cortex and piriform cortex.

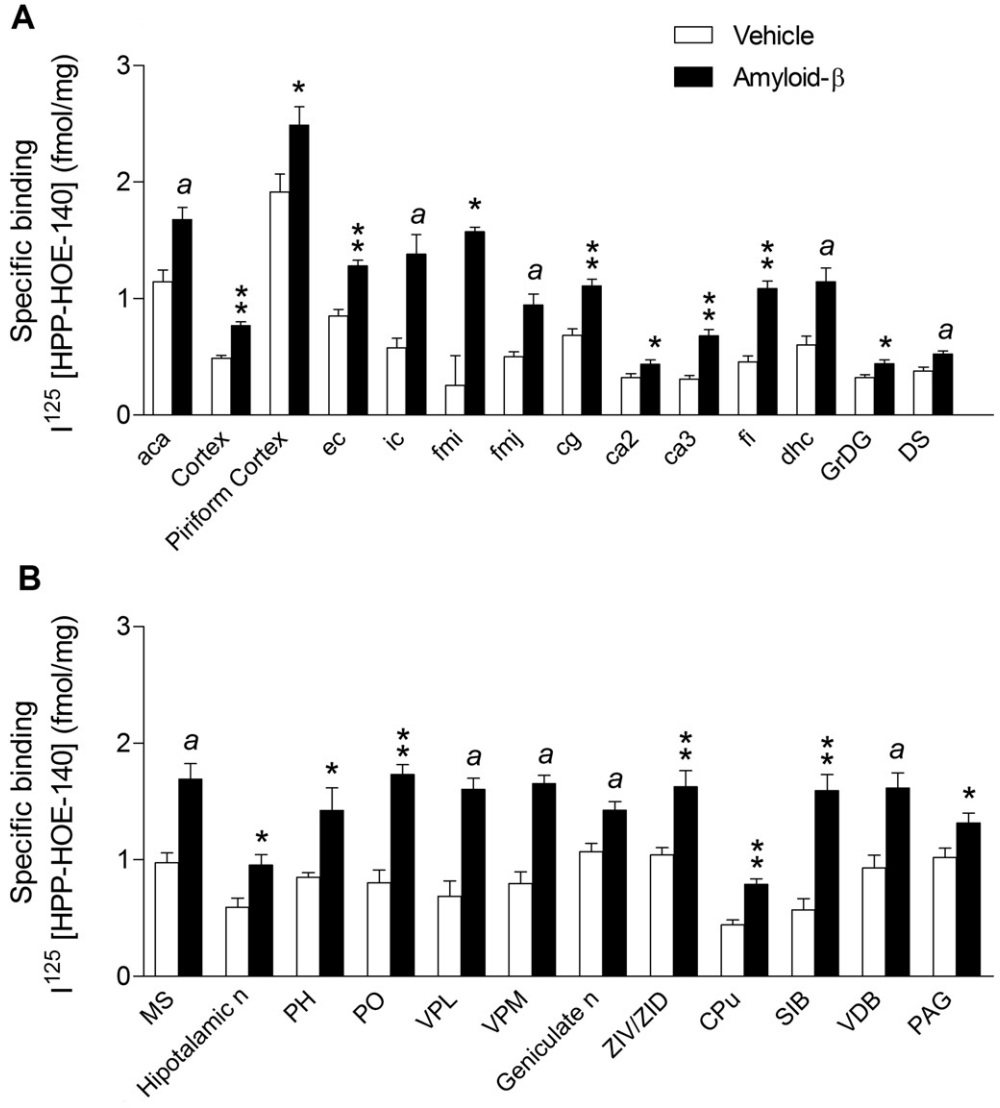

Fig. 3. Quantification of Kinin B2 receptors in KOB1 mice. Specific binding of [^{125}I]HPP-HOE 140 (200 pM, 90 min, room temperature) to B2 bradykinin receptors in different brain areas from Vehicle (blank bars, n = 6) and amyloid-β (dark bars, n = 6) of KOB1 mice groups. Data are expressed as mean ± S.E.M. *P < 0.05; ^{a}P < 0.01; **P < 0.001.

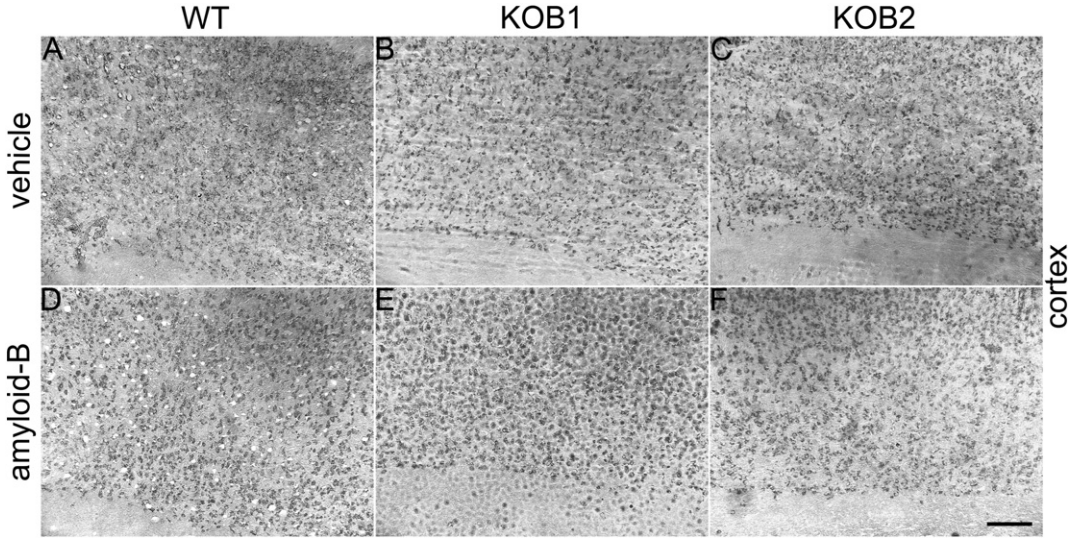

Fig. 4. Anatomical distribution of NeuN in the cortex. Representative photomicrographs of NeuN immunoreactivity from cortex of WT, KOB1 and KOB2 mice infused with Vehicle or amyloid-β. Scale bar: 80 μm. For anatomical localization, refer to panel "M" from Fig. 5.

compared to vehicle infused animals (24.1 ± 15.4% and 30.9 ± 14.7% respectively. Regarding KOB2 mice, and taking into account only vehicle-infused animals, the absence of this receptor, *per se*, promoted a decrease in neuronal bodies. In the cortex, a significant reduction of 28.5% ($P < 0.001$) was found when compared to WT animals. In the hippocampus, a reduction of 45.6% ($P < 0.05$) and 52.1% ($P < 0.01$)

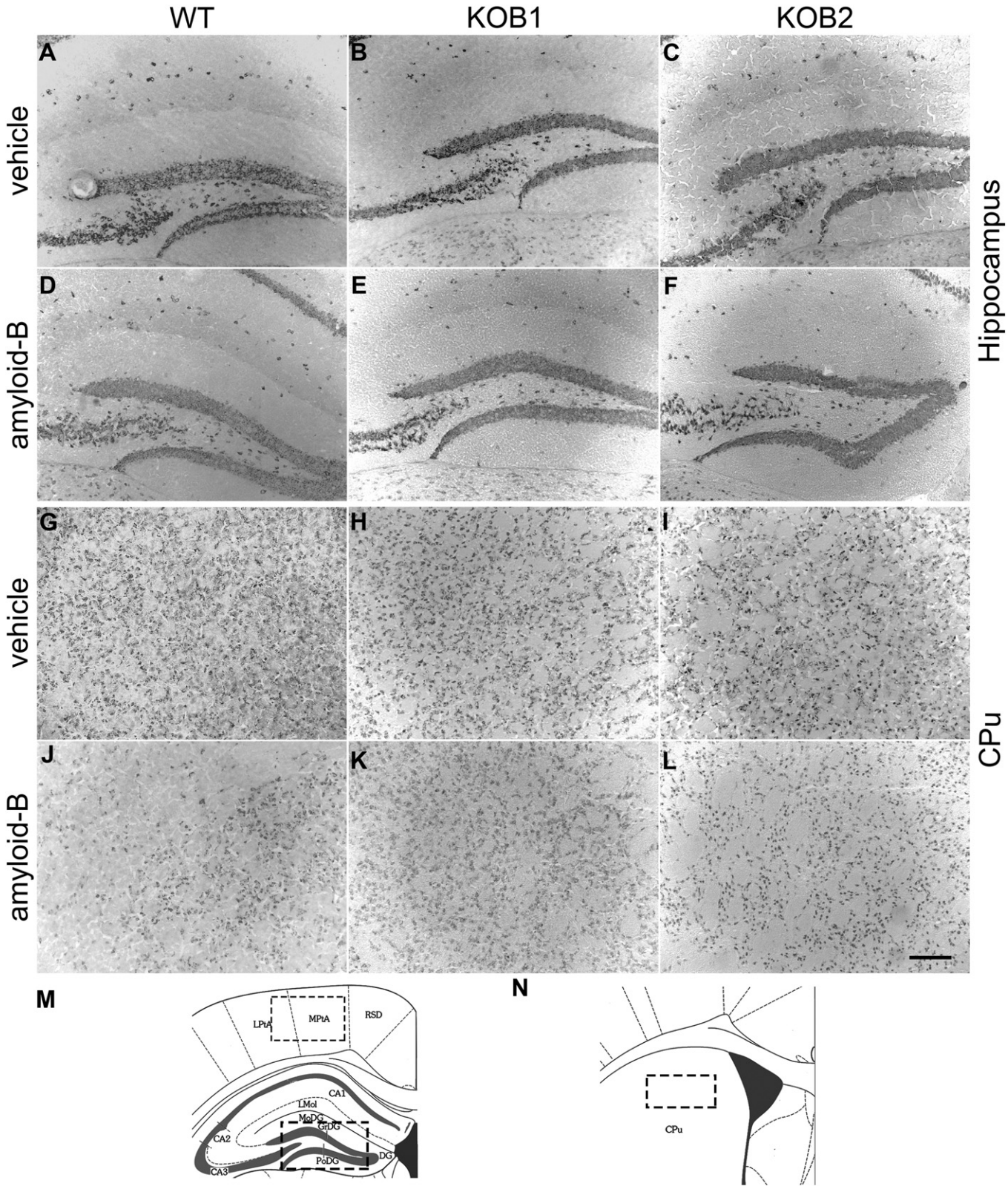

Fig. 5. Anatomical distribution of NeuN in the hippocampus and CPu. Representative photomicrographs of NeuN immunoreactivity from hippocampus and CPu of WT, KOB1 and KOB2 mice infused with Vehicle or amyloid-β. Scale bar: 80 μm. Abbreviation not cited in previous figure legends: lateral parietal association cortex, LPtA; retrosplenial dysgranular córtex, RSD; medial parietal association cortex, MPtA; lacunosum moleculare layer of the hippocampus, LMol; polymorph layer of the dentate gyrus, PoDG, and; dentate gyrus, DG.

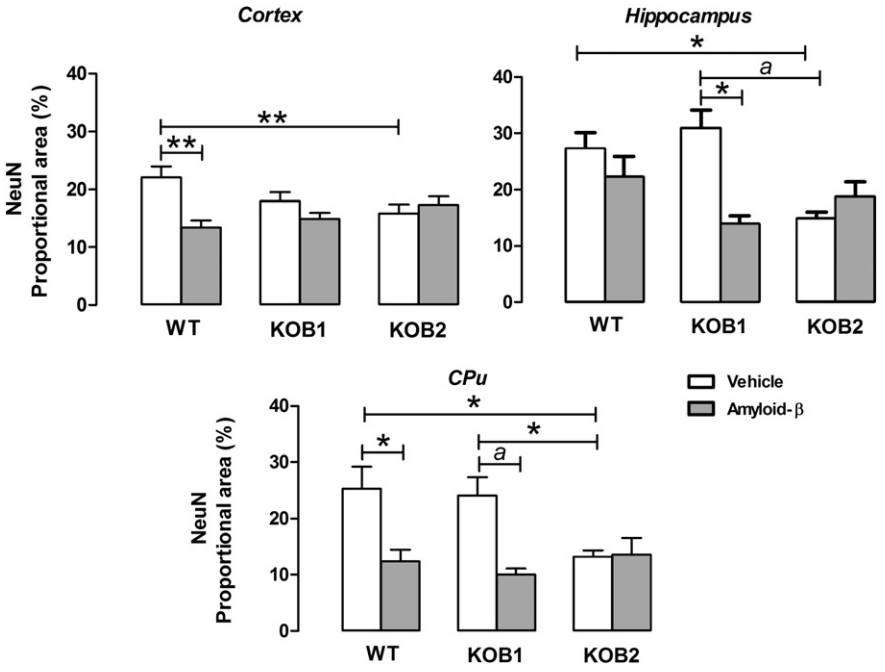

Fig. 6. Immunostaining to NeuN. Proportional area (%) occupied by immunostaining to NeuN in WT, KOB1 and KOB2 mice infused with vehicle (n = 6) or amyloid-β (n = 6). Data are expressed as mean ± S.E.M. *P < 0.05; [a]P < 0.01; **P < 0.001.

was verified in relation to WT and KOB1 animals, respectively. In the CPu, a similar profile was observed: significant reduction of 47.8% (P < 0.05) and 45.2% (P < 0.05) were verified in comparison to WT and KOB1 animals (Figs. 4, 5 and 6). Infusion of Aβ peptide did not alter NeuN labeling in brains of KOB2 mice.

Concerning the synaptic terminals, only in the cortex the absence of B2 receptors promoted a significant reduction in synaptophysin labeling in vehicle infused animals. When compared to WT animals (proportional area: 6.74 ± 0.85%) the reduction of 68.6% was verified (P < 0.001) and when compared to KOB1 animals (proportional area: 6.55 ± 0.60%), a reduction of 67.3% (P < 0.001) was verified (Figs. 7, 8 and 9). KOB2 animals infused with Aβ presented synaptic densities similar to the other groups and significantly higher (four times) than vehicle infused mice (2.14 ± 0.13%).

In the hippocampus, the absence of B2 receptors promoted a significant increase of 1.2 times (P < 0.05) and 1.5 times (P < 0.001) in synaptic terminals when compared to WT vehicle (7.54 ± 0.47%) and KOB1 vehicle (6.03 ± 0.51%) mice (Figs. 7, 8 and 9). In CPu, only vehicle-treated KOB1 mice presented significant reduction of 31.9% in synaptophysin labeling, when compared to WT vehicle-infused mice

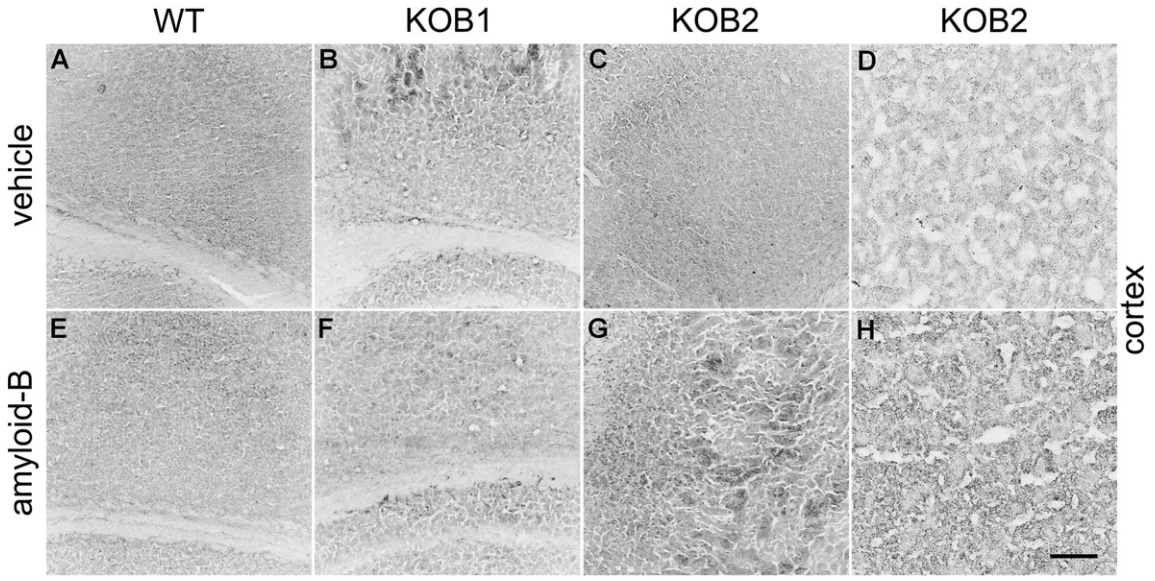

Fig. 7. Anatomical distribution of Syn2 in the cortex. Representative photomicrographs of Syn2 immunoreactivity from cortex of WT, KOB1 and KOB2 mice infused with Vehicle or amyloid-β. Panels "D" and "H" are amplification of central part of panels "C" and "G" respectively. Scale bar: 80 μm for panel "A", "B", "C", "E", "F" and "G" and 20 μm for panels "D" and "H". For anatomical localization, refer to panel "M" from Fig. 5.

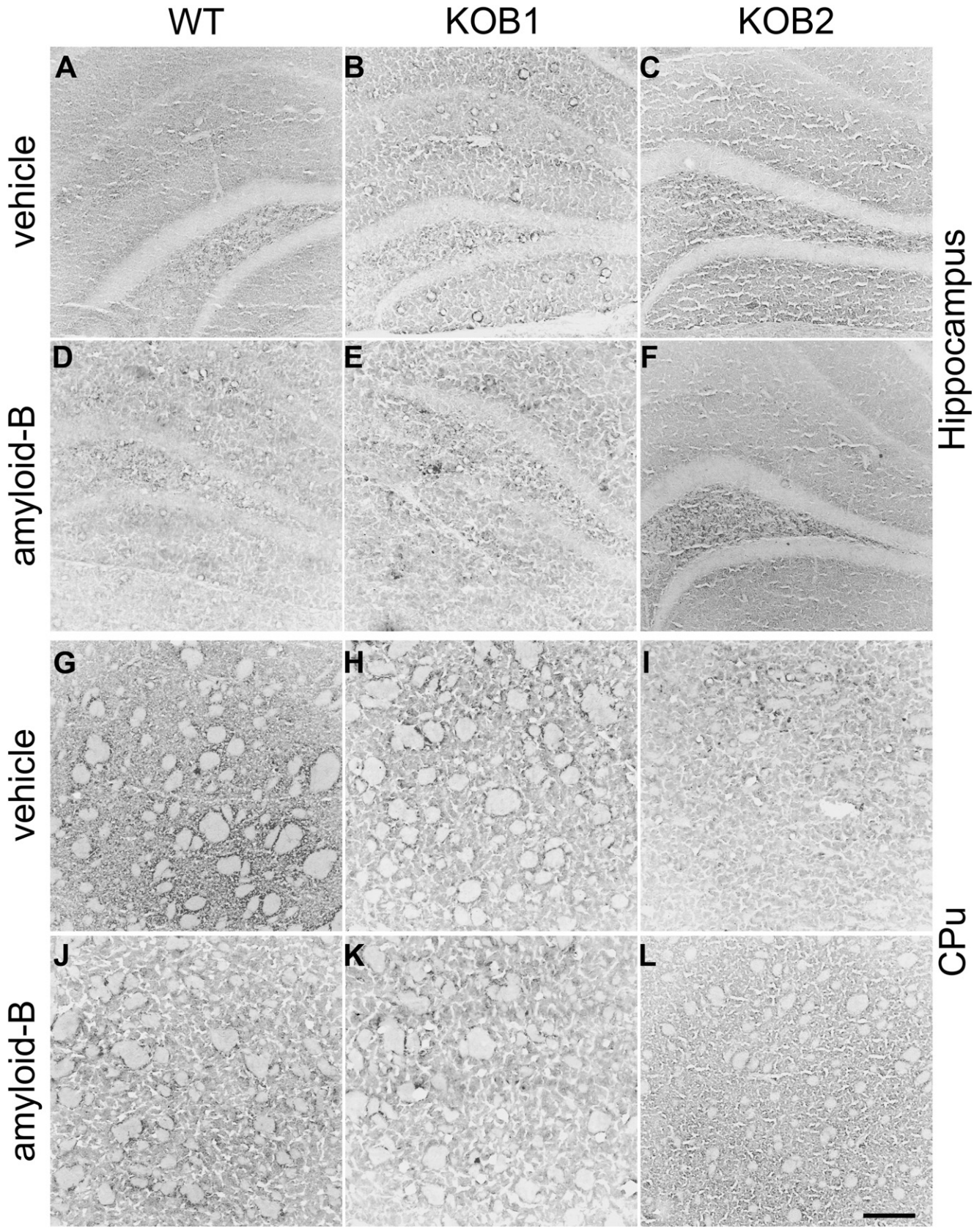

Fig. 8. Anatomical distribution of Syn2 in the hippocampus and CPu. Representative photomicrographs of Syn2 immunoreactivity from hippocampus and CPu of WT, KOB1 and KOB2 mice infused with Vehicle or amyloid-β. Scale bar: 80 μm. For anatomical localization, refer to panels "M" and "N" from Fig. 5.

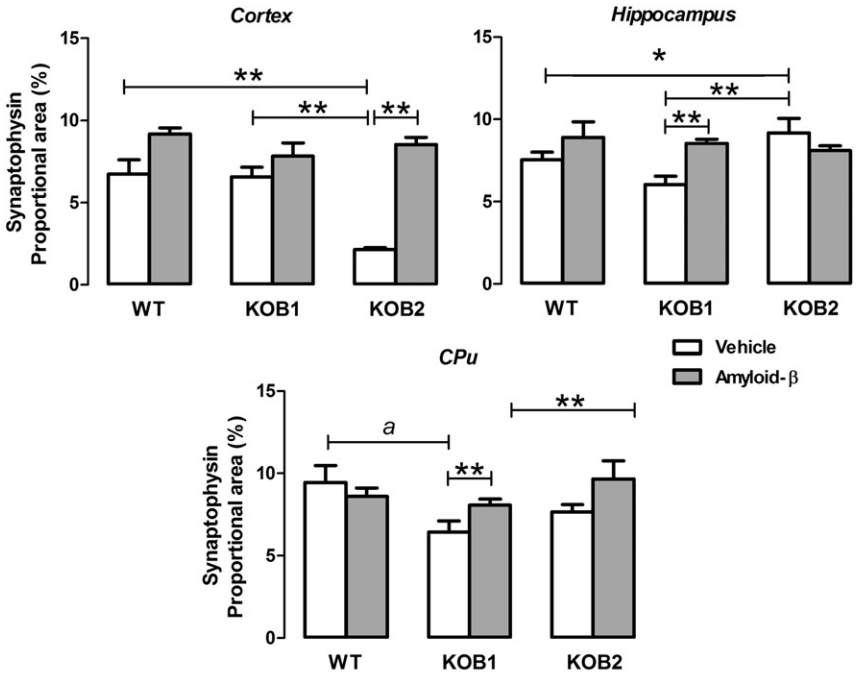

Fig. 9. Immunostaining to Syn2. Proportional area (%) occupied by immunostaining to Syn2 in WT, KOB1 and KOB2 mice infused with vehicle (n = 6) or amyloid-β (n = 6). Data are expressed as mean ± S.E.M. *P < 0.05; [a]P < 0.01; **P < 0.001.

(9.45 ± 1.03%). In the CPu and hippocampus but not in the cortex of KOB1 mice, the infusion of Aβ significantly increased the density of synaptic terminals (Figs. 7, 8 and 9).

3.4. Quantification of hippocampal deposition of amyloid plaques

In order to evaluate variations in amyloid deposits related to the different strains, Congo red staining was performed. Amyloid deposits were observed in all strains infused with Aβ peptide (Fig. 10A-B). KOB2 mice presented significant increase of 4.2 times in senile plaques density (P < 0.05) (expressed as number of plaques per number of slices) when compared to WT animals (0.04 ± 0.01%). Similarly, KOB2 mice presented significant increase of 2.83 times (P < 0.05) in this density, when compared to KOB1 animals (0.06 ± 0.02%) (Fig. 10C). The amyloid deposits were scarcely distributed in the hippocampus leading to the analyses of a large amount of slices (20–23 per animal). Almost no staining was observed in the cortex and CPu and as expected, no staining was observed in the vehicle groups.

4. Discussion

In a previous publication we showed that intraventricular infusion of Aβ in KOB2 mice promoted a significant decrease in aversive-related memory. Besides that, similar infusion in KOB1 mice did not change animals' response to memory task (Amaral et al., 2010). With these data, it was suggested that the lack of B2 receptors could contribute to neurodegeneration and loss of memory. Continuing that study and using brain samples from those animals, in the present study we show that KOB1 mice infused with Aβ presented a decrease in neuronal density in the hippocampus and CPu and an increase in synaptic densities. Nevertheless, an increase in B2 receptor density was also observed in these animals. These results offer one more evidence of the neuroprotective role of B2 receptors in neurodegenerative processes.

Kinin B1 receptor is generally associated with inflammatory responses. Induction and increase in densities of this receptor were observed in several pathological conditions, including chronic neurological diseases (Raidoo et al., 1996; Marceau et al., 1998; Prat et al., 1999; Prat et al., 2000; Prediger et al., 2008; Viel et al., 2008). Interestingly, animals lacking B1 receptors showed no cognitive deficits after Aβ chronic infusion suggesting, at first, that the absence of cognitive deficits could be due to the lack of B1R. On the other hand, KOB2 mice submitted to the same protocol showed faster cognitive deficits which could be related to the lack of B2R (Amaral et al., 2010). Similar results were observed in aged KOB1 or KOB2 mice (Lemos et al., 2010).

The *in vitro* quantitative autoradiography performed in this study showed significant increases of B2R densities in several memory related nuclei in KOB1Aβ mice and no detectable changes of B1R density in KOB2Aβ. These data led us to suggest that the absence of memory impairment in KOB1Aβ mice could be related to the increase in density of B2R and the accelerated memory impairment in KOB2Aβ to the lack of B2R. Different from what was observed in rats, apparently mice show bare distribution of central B1R in neuroinflammation (De Sousa Buck et al., 2002; Ongali et al., 2003a; Ongali et al., 2003b; Campos et al., 2005; Ongali et al., 2006; Lacoste et al., 2013), since levels were undetectable by autoradiography. This apparent interspecies differences in B1R distribution in AD animal models demands quantification and localization of this receptor in samples from human donors with neurohistopathological confirmation of AD.

Additionally, we analyzed immunoreactivity to NeuN, which is a general neuronal marker, (Colom et al., 2010) and Syn2 in the cortex, hippocampus and CPu. Syn2 is a presynaptic vesicle protein located in axons (Tarsa and Goda, 2002) and its increased level is correlated to improvement of cognitive function in rodents (Mulder et al., 2004). Here we observed a decrease in neuronal bodies after Aβ injection in WT (cortex and CPu) and in KOB1 (hippocampus and CPu) groups. In the same way, it has already been reported that the presence of Aβ 1–40 promoted a decrease of 16% in NeuN immunelabeling in CA1 area compared to control animals (Colom et al., 2011). The absence of B2 receptors decreased the neuronal density in KOB2 mice, corroborating the hypothesis that B2 receptor may play a protective role in the central nervous system in Alzheimer's disease, and its absence weakens neuronal connection, leading to the disruption in memory observed earlier with these mice (Amaral et al., 2010). Also, it should be considered that the lower baseline coverage of NeuN area in the hippocampus and the CPu of KOB2 could be due to a decrease in neurogenesis, since this receptor is also involved in this process (Martins et al., 2008; Pillat

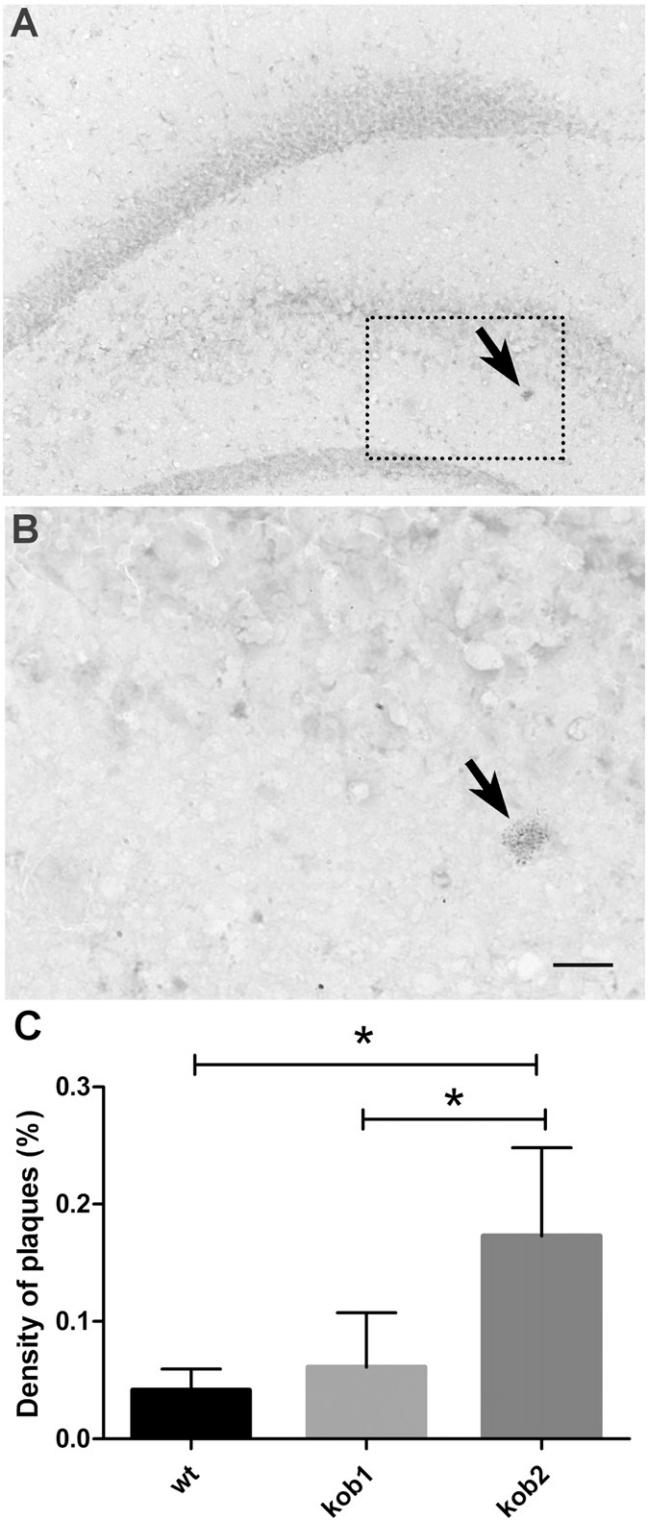

Fig. 10. Localization and distribution of Aβ deposits. Representative photomicrographs of amyloid-β deposits (A and B) of KOB2 mice infused with amyloid-β and proportional distribution (number of plaques per number of slices) of Aβ deposits (C) in C57Bl/6 (WT), KOB1 and KOB2 mice infused with Aβ peptide. Arrows on panels "A" and "B" indicates amyloid deposits. The panel "B" shows the dashed square area in "A". Scale bar is 160 μm for "A" and 40 μm for "B". Data on "C" are expressed as mean ± S.E.M. *$P < 0.05$.

et al., 2015). Besides, with the chronic infusion of Aβ peptide an increase in synaptophysin density was observed in KOB2 animals' cortex. This striking result was also observed previously after a single injection i.c.v. in animals treated with HOE 140, a specific antagonist for B2 receptor (Bicca et al., 2015). In light of all data indicating the neuroprotective role of B2 receptor, these observations regarding the increase in synapse terminals in the presence of neurodegeneration seem to be a consequence of a mechanism that may give rise to replacement of neurons lost during the disease development, as already reported earlier concerning neurogenesis in brains from AD patients and in animal models of neurodegeneration (Jin et al., 2004; López-Toledano and Shelanski, 2007; Yu et al., 2009).

Considering the hypothesis of increased B2R densities being located in astrocytes, bradykinin release could indirectly trigger a neuroprotective or a neurodegenerative stimulus. This hypothesis could explain different results obtained by Prediger et al. (2008) and Bicca et al. (2015), where B2R was suggested to be involved in the pathophysiology of AD. In the first study, the equimolar amount of Aβ peptide that we used in this study was injected in one single shot. In the second study, the pre-treatment with selective kinin B2 receptor agonist (HOE 140) followed by acute injection of Aβ inhibited neuroinflammation, reduced pro-inflammatory proteins, protect against synapsis loss and cognitive impairment in mice. In both cases acute injection of Aβ could activate an acute inflammatory process by activating phospholipase A_2 leading to formation of aracdonic acid and prostaglandins. Formation of reactive oxygen species (ROS) was also reported, increasing oxidative stress and inflammation (Thornton et al., 2010). Further studies are being done in our laboratory in order to identify the cell type containing B2R in the brain of a transgenic mice model expressing human amyloid precursor protein (APP) during aging.

Another possible explanation for the B2R function in neurons is through primarily Gq activation by B2R and to a more limited extent, also through Gi mechanism. Gq activation stimulates phospholipase Cβ (PLCβ) and phospholipase A_2 (PLA_2) (Prado et al., 2002). PLCβ activates PKC via diacyl glycerol (DAG) and microsomal Ca^{2+} release. PLA_2 initiates the release of arachidonic acid which is converted to PGE2, by cyclooxygenase (Cox) and prostaglandin synthases, and can activate PKA via E-prostanoid G-protein coupled receptors (Smith et al., 2000). PKA and PKC may phosphorylate NMDA or AMPA receptor subunits, changing the membrane traffic and their kinetic properties (voltage-dependent block, channel open time, burst behavior), triggering an increase in synaptic effectiveness (Kohno et al., 2008). Very recently, it was shown that B2R stimulation leads to neuroprotection after NMDA excitotoxicity in the CA1 area of rat hippocampal slices via phosphatidylinositol 3-kinase and not by MEK/MAPK signaling (Martins et al., 2012).

On the other hand, in mice expressing the human APP, the chronic infusion of B1 antagonist SSR240612 (for 10 weeks) abolished the amyloidosis, cerebrovascular and memory deficits providing evidence for a role of B1R in the pathogenesis of AD (Lacoste et al., 2013). It should be considered that under chronic B1R blockade BK can act preferentially on B2R, considered neuroprotective and capable of avoiding memory loss (Noda et al., 2007). Considering the data provided in the present study showing the increased B2R binding sites in KOB1Aβ mice, the neuroprotection observed by Lacoste et al. (2013) could in part be due to a possible increase in B2R densities in those mice brains. Another interesting finding of the present study was the increased Aβ deposition in KOB2Aβ mice, suggesting that B2R activation may play an important role in Aβ degradation *in vivo*. Supporting our data, it was shown that the concentration-dependent stimulation of BV2 and N9 cell lines or primary microglial cells by BK or endothelin increased the phagocytosis of Aβ by these cells (Fleisher-Berkovich et al., 2010).

5. Conclusion

In conclusion, memory preservation in KOB1Aβ, could be due to the increase in densities of B2R in several areas, including those related to memory processing, reinforcing the neuroprotective role of B2R. The increased density of Aβ plaques and earlier memory impairment in

KOB2Aβ corroborates this information. This data points to the proposition that activation of B2R can be a potential therapeutic target in AD.

Conflict of interests

We have no conflict of interests.

Acknowledgments

This work was supported by a Grant from Fundação de Amparo a Pesquisa no Estado de Sao Paulo (FAPESP 2007/04800-0 and 2013/13656-1). Dong KE is a fellowship recipient from CAPES-PROSUP, Amaral FA was a fellowship recipient from FAPESP (2009/08049-3), Monteiro-Silva KC (123695/2013-9), Pesquero JB (301896/2014-3), Araujo MS (307404/2012-9) and Buck HS (303283/2014-9) are fellowship recipients from CNPq.

References

Amaral, F.A., Lemos, M.T., Dong, K.E., Bittencourt, M.F., Caetano, A.L., Pesquero, J.B., Viel, T.A., Buck, H.S., 2010. Participation of kinin receptors on memory impairment after chronic infusion of human amyloid-β 1–40 (Aβ) peptide in mice. Neuropeptides 44, 93–97.

Bascands, J.L., Pecher, C., Rouaud, S., Emond, C., Tack, J.L., Bastie, M.J., Burch, R., Regoli, D., Girolami, J.P., 1993. Evidence for existence of two distinct bradykinin receptors on rat mesangial cells. Am J Physiol 264, F548–F556.

Bicca, M.A., Costa, R., Loch-Neckel, G., Figueiredo, C.P., Medeiros, R., Calixto, J.B., 2015. B_2 receptor blockage prevents Aβ-induced cognitive impairment by neuroinflammation inhibition. Behav. Brain Res. 278, 482–491.

Caetano, A.L., Viel, T.A., Bittencourt, M.F., Araujo, M.S., De Angelis, K., Buck, H.S., 2010. Change in central kinin B2 receptor density after exercise training in rats. Auton. Neurosci. 158 (1–2), 71–78.

Campos, M.M., Ongali, B., De Souza Buck, H., Schanstra, J.P., Girolami, J.P., Chabot, J.G., Couture, R., 2005. Expression and distribution of kinin B1 receptor in the rat brain and alterations induced by diabetes in the model of streptozotocin. Synapse 57 (1), 29–37.

Cholewinski, A.J., Stevens, G., McDermott, A.M., Wilkin, G.P., 1991. Identification of B2 bradykinin binding sites on cultured cortical astrocytes. J. Neurochem. 57, 1456–1458.

Cloutier, F., de Sousa Buck, H., Ongali, B., Couture, R., 2002. Pharmacologic and autoradiographic evidence for an up-regulation of kinin B(2) receptors in the spinal cord of spontaneously hypertensive rats. Br. J. Pharmacol. 135 (7), 1641–1654.

Cloutier, F., Ongali, B., Campos, M.M., Thibault, G., Neugebauer, W., Couture, R., 2004. Correlation between brain bradykinin receptor binding sites and cardiovascular function in young and adult spontaneously hypertensive rats. Br. J. Pharmacol. 142, 285–296.

Colom, L.V., Castañeda, M.T., Bañuelos, C., Puras, G., García-Hernández, A., Hernandez, S., Mounsey, S., Benavidez, J., Lehker, C., 2010. Medial septal beta-amyloid 1–40 injections alter septo-hippocampal anatomy and function. Neurobiol. Aging 31 (1), 46–57.

Colom, L.V., Castaneda, M.T., Hernandez, S., Perry, G., Jaime, S., Touhami, A., 2011. Intrahippocampal amyloid-β (1–40) injections injure medial septal neurons in rats. Curr. Alzheimer Res. 8 (8), 832–840.

Couture, R., Lindsey, C.J., 2000. Brain kallikrein–kinin system: from receptors to neuronal pathways and physiological functions. In: Quirion, R., Björklund, A., Hökfelt, T. (Eds.), Handbook of Chemical Neuroanatomy, Peptide Receptors 16. Elsevier Science B.V., pp. 241–300.

De Sousa Buck, H., Ongali, B., Thibault, G., Lindsey, C.J., Couture, R., 2002. Autoradiographic detection of kinin receptors in the human medulla of control, hypertensive and diabetic donors. Can. J. Physiol. Pharmacol. 80 (4), 249–257.

Fior, D.R., Martins, D.T.O., Lindsey, C.J., 1993. Localization of central pressor action of bradykinin in medulla oblongata. Am. J. Physiol. 265, H1000–H1006.

Fleisher-Berkovich, S., Filipovich-Rimon, T., Ben-Shmuel, S., Hülsmann, C., Kummer, M.P., Heneka, M.T., 2010. Distinct modulation of microglial amyloid β phagocytosis and migration by neuropeptides (i). J. Neuroinflammation 61, 11–17.

Franklin, K., Paxinos, G., 2008. The Mouse Brain. In Stereotaxic Coordinates. third ed. Academic Press, San Diego.

Fujiwara, Y., Mantione, C.R., Yamamura, H.I., 1988. Identification of B2 bradykinin binding sites in guinea-pig brain. Eur. J. Pharmacol. 15 (147(3)), 487–488.

Hoffman, W.E., Schimid, P.G., 1978. Separation of pressor and antidiuretic effects of intraventricular bradykinin. Neuropharmacology 17, 999–1002.

Huang, H.M., Lin, T.A., Sun, G.Y., Gibson, G.E., 1995. Increased inositol 1,4,5-trisphosphate accumulation correlates with an up-regulation of bradykinin receptors in Alzheimer's disease. J. Neurochem. 64 (2), 761–766.

Hunter, W.M., Greenwood, F.C., 1962. Preparation of iodine-131 labelled human growth hormone of high specific activity. Nature 194, 495–496.

Iores-Marçal, L.M., Viel, T.A., Buck, H.S., Nunes, V.A., Gozzo, A.J., Cruz-Silva, I., Miranda, A., Shimamoto, K., Ura, N., Araujo, M.S., 2006. Bradykinin release and inactivation in brain of rats submitted to an experimental model of Alzheimer's disease. Peptides 27 (12), 3363–3369.

Jin, K., Peel, A.L., Mao, X.O., Xie, L., Cottrell, B.A., Henshall, D.C., Greenberg, D.A., 2004. Increased hippocampal neurogenesis in Alzheimer's disease. Proc. Natl. Acad. Sci. U. S. A. 101 (1), 343–347.

Jong, Y.J., Dalemar, L.R., Seehra, K., Baenziger, N.L., 2002. Bradykinin receptor modulation in cellular models of aging and Alzheimer's disease. Int. Immunopharmacol. 2 (13–14), 1833–1840.

Kariya, K., Yamauchi, A., 1981. Effects of intraventricular injection of bradykinin on the EEG and the blood pressure in conscious rats. Neuropharmacology 20, 1221–1224.

Kohno, T., Wang, H., Amaya, F., Brenner, G.J., Cheng, J.K., Ji, R.R., Woolf, C.J., 2008. Bradykinin enhances AMPA and NMDA receptor activity in spinal cord dorsal horn neurons by activating multiple kinases to produce pain hypersensitivity. J. Neurosci. 28 (17), 4533–4540.

Kozlowski, M.R., Rosser, M.P., Hall, E., 1998. Identification of 3H-bradykinin binding sites in PC-12 cells and brain. Neuropeptides 12, 207–211.

Lacoste, B., Tong, X.K., Lahjouji, K., Couture, R., Hamel, E., 2013. Cognitive and cerebrovascular improvements following kinin B1 receptor blockade in Alzheimer's disease mice. J. Neuroinflammation 4 (10), 57. http://dx.doi.org/10.1186/1742–2094–10–57.

Leeb-Lundberg, L.M.F., Marceau, F., Müller-Esterl, W., Pettibone, D.J., Zuraw, B.L., 2005. International union of pharmacology. XLV. Classification of the kinin receptor family: from molecular mechanisms to pathophysiological consequences. Pharmacol. Rev. 57, 27–77.

Lemos, M.T., Amaral, F.A., Dong, K.E., Bittencourt, M.F., Caetano, A.L., Pesquero, J.B., Viel, T.A., Buck, H.S., 2010. Role of kinin B1 and B2 receptors on memory consolidation during aging process of mice. Neuropeptides 44, 163–168.

Lindsey, C.J., Buck, H.S., Fior-Chadi, D.R., Lapa, R.C.R.S., 1997. Pressor effect mediated by bradykinin in the paratrigeminal nucleus of the rat. J. Physiol. 502 (1), 119–129.

Lopes, P., Kar, S., Tousignant, C., Regoli, D., Quirion, R., Couture, R., 1983. Autoradiographic localization of [^{125}I-Tyr8]-bradykinin receptor binding sites in the guinea pig spinal cord. Synapse 15, 48–57.

López-Toledano, M.A., Shelanski, M.L., 2007. Increased neurogenesis in young transgenic mice overexpressing human APP(Sw, Ind). J. Alzheimers Dis. 12 (3), 229–240.

Ma, J.X., Wang, D.Z., Chao, L., Chao, J., 1994a. Cloning, sequence analysis and expression of the gene encoding the mouse bradykinin B2 receptor. Gene 149, 283–288.

Ma, J.X., Wang, D.Z., Ward, D.C., Chen, L., Dessai, T., Chao, J., Chao, L., 1994b. Structure and chromosomal localization of the gene (BDKRB2) encoding human bradykinin B2 receptor. Genomics 23, 362–369.

Marceau, F., Hess, J.F., Bachvarov, D.R., 1998. The B1 receptors for kinins. Pharmacol. Rev. 50 (3), 357–386.

Martins, A.H., Alves, J.M., Perez, D., Carrasco, M., Torres-Rivera, W., Eterović, V.A., Ferchmin, P.A., Ulrich, H., 2012. Kinin-B2 receptor mediated neuroprotection after NMDA excitotoxicity is reversed in the presence of kinin-B1 receptor agonists. PLoS One 7 (2), e30755. http://dx.doi.org/10.1371/journal.pone.0030755.

Martins, A.H., Alves, J.M., Trujillo, C.A., Schwindt, T.T., Barnabé, G.F., Motta, F.L., Guimaraes, A.O., Casarini, D.E., Mello, L.E., Pesquero, J.B., Ulrich, H., 2008. Kinin-B2 receptor expression and activity during differentiation of embryonic rat neurospheres. Cytometry A 73 (4), 361–368. http://dx.doi.org/10.1002/cyto.a.20519.

Mathis, S.A., Criscimagna, N.L., Leeb-Lundberg, L.M.F., 1996. B1 and B2 kinin receptors mediate distinct patterns of intracellular Ca2+ signaling in single cultured vascular smooth muscle cells. Mol. Pharmacol. 50, 128–139.

Mulder, M., Jansen, P.J., Janssen, B.J., van de Berg, W.D., van der Boom, H., Havekes, L.M., de Kloet, R.E., Ramaekers, F.C., Blokland, A., 2004. Low-density lipoprotein receptor knockout mice display impaired spatial memory associated with a decreased synaptic density in the hippocampus. Neurobiol. Dis. 16, 212–219.

Murone, C., Paxinos, G., McKinley, M.J., Oldfield, B.J., Muller-Esterl, W., Mendelsohn, F.A., Chai, S.Y., 1997. Distribution of bradykinin B2 receptors in sheep brain and spinal cord visualized by *in vitro* autoradiography. J. Comp. Neurol. 381, 203–218.

Nazarali, A.J., Gutkind, J.S., Saavedra, J.M., 1989. Calibration of ^{125}I-polymer standards with ^{125}I-brain paste standards for use in quantitative receptor autoradiography. J. Neurosci. Methods 30 (3), 247–253.

Noda, M., Kariura, Y., Pannasch, U., 2007. Neuroprotective role of bradykinin because of the attenuation of pro-inflammatory cytokine release from activated microglia. J. Neurochem. 101, 397–410.

Okada, Y., Tuchiya, Y., Yagyu, M., Kozawa, S., Kariya, K., 1977. Synthesis of bradykinin fragments and their effect on pentobarbital sleeping time in mouse. Neuropharmacology 16, 381–383.

Ongali, B., Buck, H de S., Cloutier, F., Legault, F., Regoli, D., Lambert, C., Thibault, G., Couture, R., 2003a. Chronic effects of angiotensin-converting enzyme inhibition on kinin receptor binding sites in the rat spinal cord. Am. J. Physiol. Heart Circ. Physiol. 284 (6), H1949–H1958.

Ongali, B., Campos, M.M., Bregola, G., Rodi, D., Regoli, D., Thibault, G., Simonato, M., Couture, R., 2003b. Autoradiographic analysis of rat brain kinin B1 and B2 receptors: normal distribution and alterations induced by epilepsy. J. Comp. Neurol. 461 (4), 506–519.

Ongali, B., Hellal, F., Rodi, D., Plotkine, M., Marchand-Verrecchia, C., Pruneau, D., Couture, R., 2006. Autoradiographic analysis of mouse brain kinin B1 and B2 receptors after closed head trauma and ability of anatibant mesylate to cross the blood–brain barrier. J. Neurotrauma 23 (5), 696–707.

Pillat, M.M., Cheffer, A., de Andrade, C.M., Morsch, V.M., Schetinger, M.R., Ulrich, H., 2015. Bradykinin-induced inhibition of proliferation rate during neurosphere differentiation: consequence or cause of neuronal enrichment? Cytometry A http://dx.doi.org/10.1002/cyto.a.22705.

Prado, G.N., Taylor, L., Zhou, X., Ricupero, D., Mierke, D.F., Polgar, P., 2002. Mechanisms regulating the expression, self-maintenance, and signaling-function of the bradykinin B2 and B1 receptors. J. Cell. Physiol. 193, 275–286.

Prat, A., Biernacki, K., Pouly, S., Nalbantoglu, J., Couture, R., Antel, J., 2000. Kinin B1 receptor expression and function on human brain endothelial cells. J. Neuropathol. Exp. Neurol. 59, 896–906.

Prat, A., Weinrib, L., Becher, B., Poirier, J., Duquette, P., Couture, R., Antel, J.P., 1999. Bradykinin B1 receptor expression and function on T lymphocytes in active multiple sclerosis. Neurology 53, 2087–2092.

Prediger, R.D., Medeiros, R., Pandolfo, P., Duarte, F.S., Passos, G.F., Pesquero, J.B., Campos, M.M., Calixto, J.B., Takahashi, R.N., 2008. Genetic deletion or antagonism of kinin B(1) and B(2) receptors improves cognitive deficits in a mouse model of Alzheimer's disease. Neuroscience 151 (3), 631–643.

Raidoo, D.M., Ramchurren, N., Naidoo, Y., Naidoo, S., Müller-Esterl, W., Bhoola, K.D., 1996. Visualisation of bradykinin B2 receptors on human brain neurons. Immunopharmacology 33, 104–107.

Regoli, D., Barabe, J., 1980. Pharmacology of bradykinin and related kinins. Pharmacol. Rev. 32, 1–46.

Regoli, D., Nsa Allogho, S., Rizzi, A., Gobeil, F.J., 1998. Bradykinin receptors and their antagonists. Eur. J. Pharmacol. 348 (1), 1–10.

Sharif, N.A., Whiting, R.L., 1991. Identification of B2-bradykinin receptors in guinea pig brain regions, spinal cord and peripheral tissues. Neurochem. Int. 18, 89–96.

Smith, J.A.M., Davis, C.L., Burgess, G.M., 2000. Prostaglandin E2-induced sensitization of bradykinin-evoked responses in rat dorsal root ganglion neurons is mediated by cAMP-dependent protein kinase A. Eur. J. Neurosci. 12, 3250–3258.

Smith, J.A.M., Webb, C., Holford, J., Burgess, G.M., 1995. Signal transduction pathways for B1 and B2 bradykinin receptors in bovine pulmonary artery endothelial cells. Mol. Pharmacol. 47, 525–534.

Tarsa, L., Goda, Y., 2002. Synaptophysin regulates activity dependent synapse formation in cultured hippocampal neurons. Proc. Natl. Acad. Sci. U. S. A. 99, 1012–1016.

Thornton, E., Ziebell, J.M., Leonard, A.V., Vink, R., 2010. Kinin receptor antagonists as potential neuroprotective agents in central nervous system injury. Molecules 15 (9), 6598–6618.

Viel, T.A., Buck, H.S., 2011. Kallikrein–kinin system mediated inflammation in Alzheimer's disease in vivo. Curr. Alzheimer Res. 8 (1), 59–66.

Viel, T.A., Lima Caetano, A., Nasello, A.G., Lancelotti, C.L., Nunes, V.A., Araujo, M.S., Buck, H.S., 2008. Increases of kinin B1 and B2 receptors binding sites after brain infusion of amyloid-beta 1–40 peptide in rats. Neurobiol. Aging 29 (12), 1805–1814.

Wang, Q., Wang, J., 2002. Injection of bradykinin or cyclosporine A to hippocampus induces Alzheimer-like phosphorylation of Tau and abnormal behavior in rats. Chin. Med. J. 115 (6), 884–887.

Yu, Y., He, J., Zhang, Y., Luo, H., Zhu, S., Yang, Y., Zhao, T., Wu, J., Huang, Y., Kong, J., Tan, Q., Li, X.M., 2009. Increased hippocampal neurogenesis in the progressive stage of Alzheimer's disease phenotype in an APP/PS1 double transgenic mouse model. Hippocampus 12, 1247–1253.

Zhao, W.Q., Ravindranath, L., Mohamed, A.S., Zohar, O., Chen, G.H., Lyketsos, C.G., Etcheberrigaray, R., Alkon, D.L., 2002. MAPkinase signaling cascade dysfunction specific to Alzheimer's disease in fibroblast. Neurobiol. Dis. 11 (1), 166–183.